Polymer 324 (2025) 128228

Contents lists available at ScienceDirect

Polymer

journal homepage: www.elsevier.com/locate/polymer

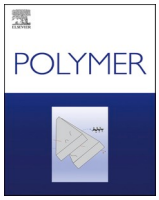

A kinetic and mechanistic study of copper-based catalysts in the ARGET-ATRP of multifunctional natural molecules: The case of methacrylated eugenol

Aniello Vittore [a], Orlando Santoro [a], Mirko Candida [b], Stefano Vaghi [b], Stefania Pragliola [c], Massimo Mella [b,*], Lorella Izzo [a,**]

[a] Dipartimento di Biotecnologie e Scienze Della Vita, Università Degli Studi Dell'Insubria, Via J.H. Dunant 3, 21100, Varese, Italy
[b] Dipartimento di Scienza Ed Alta Tecnologia, Università Degli Studi Dell'Insubria, Via Valleggio 11, 22100, Como, Italy
[c] Dipartimento di Chimica e Biologia "A. Zambelli", Università Degli Studi di Salerno, Via Giovanni Paolo II 132, 84084, Fisciano, Italy

A B S T R A C T

Herein we report on a kinetic study of Cu-based catalysts employed in the ARGET-ATRP of the methacrylic derivative of eugenol, namely eugenyl methacrylate (**EuMA**). Polymerizations were carried out in solution in presence of catalytic systems formed *in situ* by $CuBr_2$ and nitrogen-ligands such as BiPy, PMDETA, HMTETA and Me_6TREN. The formation of insoluble polymers, due to secondary reactions responsible of cross-linking, was observed with $CuBr_2$/BiPy and $CuBr_2$/HMTETA systems; Me_6TREN- and PMDETA-based catalyst proved, instead, to be capable of generating linear polymers. For the latter, first order kinetics occurred for monomer conversion up to ca 50 %, whilst higher conversion led to deviations from the linear trend. This suggested the direct involvement of the allyl group in the termination reactions, which was convincedly demonstrated by comparing kinetic results for **EuMA** and the corresponding di-hydrogenated monomer (**DEuMA**). At **EuMA** conversion above 50 %, the side reactions lead to inactivation of the PMDETA-based catalytic system via reducing agent consumption rather than to the formation of insoluble/crosslinked polymers.

Electronic structure calculations provided the energy profile for all possible side reactions. Among these, the radical chain transfer to the allyl group through hydrogen abstraction, as well as the attack of the propagating methacrylic radical to the allyl group, contributed to rationalizing the experimental behavior of the three copper-catalyst systems employed in this work.

This study demonstrates that modulating the kinetic of polymerization by properly selecting ligands and reaction temperatures represents a useful strategy towards the reduction of undesired secondary reactions of molecules with sensitive functional groups such as bio-derived phenols; moreover, such preserved functional groups would serve as possible post-functionalization sites (i.e. epoxidation) allowing for the preparation of new materials with tailored properties.

1. Introduction

The availability of molecules from renewable sources or from biomass is fostering the synthesis of new and sustainable plastics aiming at replacing those deriving from petroleum sources. Natural molecules are, however, often multifunctional and not easily polymerizable. The latter aspect can be circumvented by the introduction of polymerizable groups making such building blocks good candidates for the synthesis of new polymers; the presence of additional and reactive functional groups may, instead, represent a more serious limitation from a synthetic point of view. Despite such difficulties, the additional substituents may, in principle, be advantageously exploited as post-functionalization sites to produce added-value biobased multifunctional polymers if they remain unreacted during the polymerization process.

Biobased phenols are attractive building blocks due to the presence of aromatic rings conferring high mechanical- and thermal stability to their corresponding hypothetical novel thermoplastics. In this scenario, eugenol (**Eu**) has emerged as a promising candidate for bio-derived monomers due to its natural abundance as well as for the possibility of being obtained from biomass valorization (i.e. lignin depolymerization) [1–4]. The radical polymerization of **Eu** is generally not occurring despite the presence of an allyl group on the aromatic ring due to the poor reactivity of said function and the radical scavenger action of the phenolic group; hence, eugenol-based polymers are generally obtained by radical polymerization following introduction of an acrylic- or methacrylic polymerizable moiety via esterification of the phenylic group. However, the presence of the allyl double bond may, unfortunately, hamper the growth of linear chains during polymerization, as the

* Corresponding author.
** Corresponding author.
E-mail addresses: massimo.mella@uninsubria.it (M. Mella), lorella.izzo@uninsubria.it (L. Izzo).

https://doi.org/10.1016/j.polymer.2025.128228
Received 14 November 2024; Received in revised form 26 February 2025; Accepted 2 March 2025
Available online 3 March 2025

formation of radicals involved in inter- and intra-chain bond formation processes can still occur. In fact, literature reports describe the use of allyl-containing monomers based on eugenol mainly in the production of thermosetting polymers [5,6], [7] [8,9].

Although eugenol has been mainly employed as a self-curing monomer, the formation of linear chains and the preservation of the allyl double bonds would be an advantage, as the latter could be employed in post-functionalization reactions and converted into functional groups (i.e. epoxy or cyclic carbonate) able to react with a wide range of reactants to produce materials with targeted properties, branched or hyperbranched copolymers or simply to tune properties of the final product through controlled cross-linking reactions.

In this respect, the reactivity of several saturated- and unsaturated eugenol derivatives has been compared in a recent investigation on free radical polymerizations by Molina-Gutierrez et al. [10] They found that ethoxyeugenyl methacrylate (**EEMA)** and ethoxyisoeugenol methacrylate (**EIMA**) were interested by secondary reactions responsible for the decreasing of the propagation rate and of the consumption of about 9 and 15 % of the allyl and propenyl moieties respectively. The secondary reactions were attributed to the abstraction of a hydrogen from the α-carbon of the allyl and propenyl groups leading to a resonance-stabilized radical species and/or to the involvement of the allyl and propenyl double bond in the radical addition. [11,12]. It was also suggested that the increase of molar masses and polydispersity within the 24 h of polymerization (>3 or multimodal dispersion for *poly*-(**EIMA**) and *poly*-(**EEMA**), respectively) reflected the formation of branched polymers in both cases. Furthermore, the higher reaction rate of **EIMA** compared to that of **EEMA** indicated the higher propensity of propenyl groups for cross-propagation rather than hydrogen-abstraction [13], with the latter reaction being responsible for the formation of a stable and poorly reactive radical.

At the best of our knowledge, no studies have been reported so far on the influence of allyl reactivity in the eugenyl derivatives polymerization via controlled radical processes. Herein, we focused our studies on Activators ReGenerated by Electron Transfer - Atom Transfer Radical Polymerization (ARGET-ATRP) [14] to establish how the energetics of radical species produced during the process, and here evaluated from electronic structure calculations, can influence the chain propagation of eugenyl methacrylate (**EuMA**) in the presence of three copper-based catalysts with different activity. ARGET polymerization was chosen due to the low catalyst loadings employed and for its controlled/living character; besides, ARGET could, at least in principle, limit the occurrence of secondary reactions involving the allyl moiety featured on the monomer and would also afford polymers with terminal chain active for further radical growing processes, thus paving the way to novel block copolymers with target properties. In the following, we thus report the electronic structure calculations of the radical species that can be produced during the polymerization and their possible evolution during the growing chain steps. The energetics of the secondary reactions were compared to that of methacrylate-methacrylate propagation to evaluate their competitiveness with respect to the latter. The results obtained by the theoretical studies have been used to rationalize the experimental polymerization behavior of $CuBr_2$/L (L = BiPy, HMTETA, PMDETA) catalytic systems characterized by different k_{act}/k_{deact} in the ATRP.

2. Experimental section

2.1. Materials

All manipulations involving air-sensitive compounds were carried out under nitrogen atmosphere using standard Schlenk techniques. Eugenol, methacrylic anhydride, anisole, 4-(dimethylamino)pyridine (DMAP), *N*,*N*,*N*′,*N*″,*N*″ pentamethyldiethylenetriamine (PMDETA), 2,2′-bipyridyl (BiPy), 1,1,4,7,10,10-hexamethyltriethylenetetramine (HMTETA), Tris [2-(dimethylamino)ethyl]amine (Me_6TREN) and ethyl α-bromoisobutyrate (EBIB) were purchased from TCI chemicals; Dihydroeugenol, Copper (II) Bromide ($CuBr_2$), $Sn(oct)_2$, *N*,*N*-Dimethyl formamide (DMF), ethyl acetate, Na_2SO_4, Methyl methacrylate (**MMA**), CH_2Cl_2 and petroleum ether were purchased from Merk. Anisole and DMF were dried on $CaCl_2$ and Na_2CO_3, respectively. All other chemicals were used as received.

2.2. Methods

Eugenyl methacrylate (**EuMA**) and dihydrogeneugenyl methacrylate (**DEuMA**) were synthesized applying DMAP and methacrylic anhydride method according to a reported procedure [15].

2.2.1. ARGET-ATRP polymerizations

In a typical procedure, a degassed and N_2 backfilled Schlenk flask equipped with a magnetic stir bar was charged with anisole (1 mL, 1/1 v/wt with respect to monomer), $CuBr_2$ 27 μL (0.5 M in DMF, 0.011 mmol, 1 equiv.), Ligand 43 μL (0.5 M in DMF, 0.022 mmol, 2 equiv.), **EuMA** (1.0 g, 4.3 mmol, 400 equiv.) EBIB 16 μL (10 equiv.) and $Sn(oct)_2$ 43 μL (0.5 M in anisole, 2 equiv.). The flask was placed in an oil bath thermostated at 60 °C and stirred for the desired time. The reaction was quenched upon venting the vessel, the crude mixture was diluted with acetone (2 mL) and the product was precipitated in petroleum ether (60 mL), recovered by filtration and dried at 60 °C in vacuum for 16 h.

2.2.2. Synthesis of P(EuMA-b-MMA) copolymer: using P(EuMA) as macroinitiator for chain extension

A degassed and N_2 backfilled Schlenk flask equipped with a magnetic stir bar was charged with anisole (0.5 mL), P**(EuMA)** (0.050 g), $CuBr_2$ 2 μL (0.4 M in DMF, 1 equiv.), PMDETA 3.2 μL (0.5 M in DMF, 2 equiv.), **MMA** (0.20 g, 2.0 mmol, 2500 equiv.) and $Sn(oct)_2$ 16 μL (0.5 M in anisole, 10 equiv.). The flask was placed in an oil bath thermostated at 80 °C and stirred for 4 h. The reaction was quenched upon venting the vessel, the crude mixture was diluted with acetone (1 mL) and the product was precipitated in petroleum ether (60 mL), recovered by filtration and dried at 60 °C in vacuum for 16 h.

2.2.3. Characterization

^{1}H- and ^{13}C-{^{1}H} NMR spectra were recorded at 25 °C on a Bruker AV400 spectrometer operating at 400 and 100 MHz for ^{1}H and ^{13}C, respectively, in deuterochloroform. Spectra were calibrated against the residual portion impurity of the deuterated solvent.

ATR-FTIR spectra were recorder on a Cary 630 FTIR spectrometry (Agilent Technologies) at room temperature with 16 scans and a resolution of 4 cm^{-1}.

M_n and Đ values were determined against polystyrene standards by GPC analyses performed on a modified Jasco HPLC equipped with a Shodex KF-804 L column, operating at 30 °C in THF with a flow rate of 1 mL/min.

Thermal characterization was performed by Stare system DSC 3 (Mettler Toledo) and by Stare system TGA 2 (Mettler Toledo). DSC samples were heated from 25 to 150 °C, cooled down to 0 °C and heated again to 150 °C at a rate of 10 °C/min, using 50 mL/min nitrogen flow rate. The glass transition temperatures (T_g) were determined from the second heating ramp. The thermal degradation properties were investigated by heating the sample from 25 to 600 °C at a rate of 10 °C/min in a nitrogen atmosphere.

2.2.4. Electronic structure calculations

The reactivity of the various functional groups that could be involved during the radicalic polymerization of **EuMA** was investigated employing electronic structure calculations at the B3LYP/LANL2DZ level of theory as implemented in the Gaussian09 suite of codes [16]. Minimum energy geometries were fully optimized and characterized by means of vibrational frequency calculations; relaxed scans along selected internal coordinates were employed to locate approximate transition state (TS) structures, which were subsequently optimized and

characterized as done for minimum energy geometries.

3. Results and discussions

To produce polymers via chain polymerization processes from eugenol, the introduction of a polymerizable part such as a the methacrylic moiety is required, as the allyl double bond proved to be substantially inactive in direct polymerizations (*vide infra*, however, for further details). This notwithstanding, the allyl group can interact with the methacrylic growing chain of eugenyl methacrylate via two alternative modes during propagation (Scheme 1) [7,8].

a) α-hydrogen abstraction from the allyl moiety leading to a poorly reactive radical stabilized by resonance;
b) addition to the allyl group generating a novel propagating species, the unpaired electron being borne by a secondary carbon atom.

We carried out electronic structure calculations on both primary and secondary reactions to gain a wider understanding of the reactivity involved during radical polymerization of **EuMA**. In doing this, we considered that the thermodynamic stability of intermediates, as well as their reactivity toward monomer addition, are crucial in the definition of the extent of the involvement of allyl groups into the growing-chain reaction.

3.1. Electronic structure calculations

To begin our theoretical exploration, we carried out electronic structure calculations on the reactivity of methacrylic propagating species with respect to methacrylates and the allyl functional group. Since the initiation step, meaning the formation of the first propagating radical generated from the initiator, preferentially occurs on the methacrylic group, Scheme 2 reports the energy profiles of reactions that conserve the presence of a reactive radical and, thus, should foster chain propagation.

As for the attack by the **EuMA** radical to the methacrylic C═C double bond (involving **TS1** and **P1**), the calculations clearly indicate the methacrylic-methacrylic bond formation to be substantially exothermic and energetically unhindered, an expected finding as the process substitutes the weaker π-type covalent bond with a σ-type one while maintaining the tertiary nature of the unpaired electron-bearing carbon atom. The nature of the final product changes, instead, when the **EuMA** radical attacks the allyl double bond (involving **TS3** and **P3**), an event that generates a secondary, non-mesomerically stabilized, radical as final product; the latter observation fully rationalizes the decreased exothermicity (by roughly 6 kcal/mol) and higher energy barrier that needs to be surmounted for the reaction to take place. Finally, **EuMA** radical may abstract one of the two hydrogen atoms in α position with respect to the phenyl ring and allyl double bond (**TS2** and **P2**), forming a secondary radical that may, however, be stabilized with respect to the methacrylic counterpart by the conjugation with both unsaturated functional groups. The energetic effect of the latter is made clear by the results in Scheme 2, which indicate a much lower (roughly 14 kcal/mol) electronic energy for the products than for the reagents and a potentially less marked reactivity of the produced radical against typical reactions (*vide infra* for further details). Worth a notice, **TS2** is located 5.5 kcal/mol above the reactants, an energy barrier that, albeit being roughly seven to eight times higher than the average value of the thermal energy at temperatures (60–90 °C) commonly used for ATRP-like processes, may still be surmounted with sufficiently high frequency to impact on the overall reactivity of **EuMA**.

The possible generation of **P2** and **P3** in the reaction environment during chain propagation may have several effects impacting on the desired linear polymerization involving exclusively the methacrylic radical/methacrylate pair. In fact, both of **P2** and **P3** species may be starting points (i.e. initiators) for a side chain growth, which would generate branched species if the **Eu** group in **P2** and **P3** was attached to an already formed chain. We have, therefore, investigated the reactivity of the latter radicals with the active functional groups present in all species; these results are discussed in some detail in the Supporting Information file. For the sake of the ensuing discussion, we indicate that all investigated processes need to surmount substantially higher energy barriers compared to the desired chain propagation via attack by a methacrylic radical onto a methacrylate double bond.

Overall, the results emerging from electronic structure calculations indicate that the addition of a monomer to the methacrylic radical preferentially occurs through the methacrylic group, even if secondary reactions involving the allyl group have accessible energetics. In particular, a sufficiently high concentration of growing radical chains may foster both branching and crosslinking of chains, with effects that may vary from an increase in polydispersity index to the formation of insoluble materials. Given the lowest reaction barrier presented by the addition of a methacrylic radical to a methacrylate, it is straightforward to indicate that low temperatures ought to be employed to limit the parasitic reactions leading to **P2** and **P3**. In practice, lowering the operational temperature is expected to be more effective in reducing the

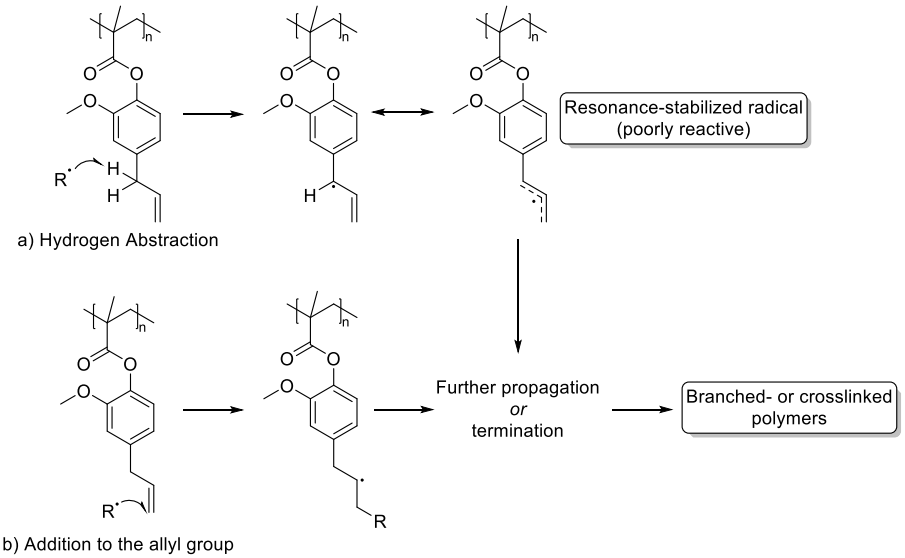

Scheme 1. Possible reactions between the propagating polymerization species and the allyl group of **EuMA** [7, 8].

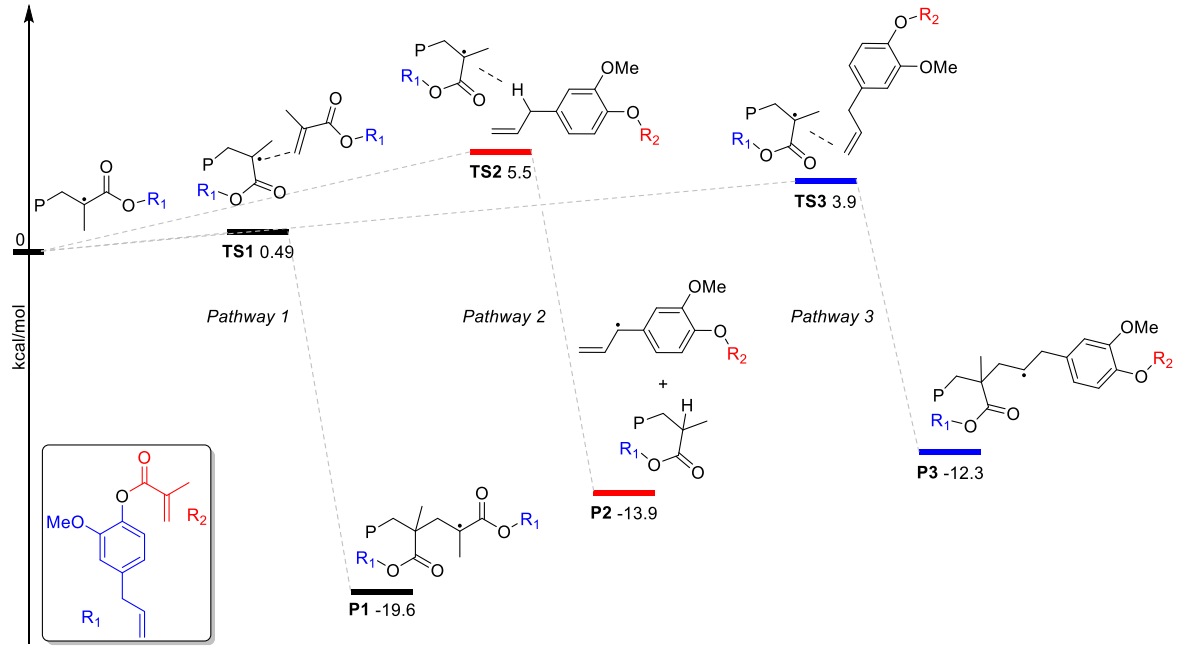

Scheme 2. Main possible reaction pathways starting from the **EuMA** radical. A common electronic energy zero is chosen to simplify comparison, and it is taken to be equal to be a simplified model for the propagating chain (i.e. the **EuMA** radical with P═H) plus the reactive counterparts.

production of **P2** compared to **P3**; it should thus stop, or at least limit, the generation of **P2a**, **P2b**, **P2c** and **P2d** (See the Supporting Information, Fig. S10). This notwithstanding, it is important to notice that high radical concentration, such as one obtained in free radical polymerization, together with the increasingly higher relative number of allyl groups compared to the methacrylic ones that is left in the reaction mixture as time elapses, might favor reactions involving the allyl moiety rather than the methacrylic propagation.

3.2. *ARGET-ATRP polymerizations*

As an alternative (or juxtaposing) to the usage of low temperatures, which would also reduce the overall polymerization kinetics, controlled radical polymerization methods such as ATRP may limit side reactions. In fact, in the ATRP techniques, the activation-deactivation mechanism of the metal catalyst in different oxidation states $\mathbf{M^nXL_n/M^{n+1}X_2L_{n\text{-}1}}$ determines the concentration of radicals during the polymerization process, with the equivalents of the metal complex in the lowest oxidation state corresponding to the amount of the dormant species P_m-X (Scheme 3).

If dormant species are less likely to be reactivated following the reforming of halogenated species, they would generate a lower concentration of radicals compared to what is obtained from the halogenated form of **P1**.

In this respect, the secondary radical nature of species **P3**, juxtaposed with the absence of radical stabilizing groups via mesomeric effects, may be expected to afford lower activation rates (k_{act}) [17], as previously indicated in the literature, than the one expected for the dormant species deriving from **P1**, the most convenient outcome for our aim being the possibility that, *de facto*, **P3** would represent "a sink" for chain propagation. This is expected to be the case if the dormant species associated with **P3** required a substantially higher bond dissociation energy (BDE) to homolytically lose the halogen compared to the one related to **P1** [18]. We have thus investigated this aspect via electronic structure calculations and, indeed, it appears to be the case, as is indicated by the fact that the change in electronic energy, obtained with our DFT approach, for the reaction

$$\boldsymbol{P1} - Br + \boldsymbol{P3} \rightarrow P1 + \boldsymbol{P3} - Br$$

is indeed negative by −16.1 kcal/mol, a direct consequence of a higher BDE for **P3**–Br.

Species forming from the reattachment of a bromine atom to **P2**, instead, may be reactivated more rapidly due to their relative stability even compared to the formation of the tertiary methacrylic radical, in

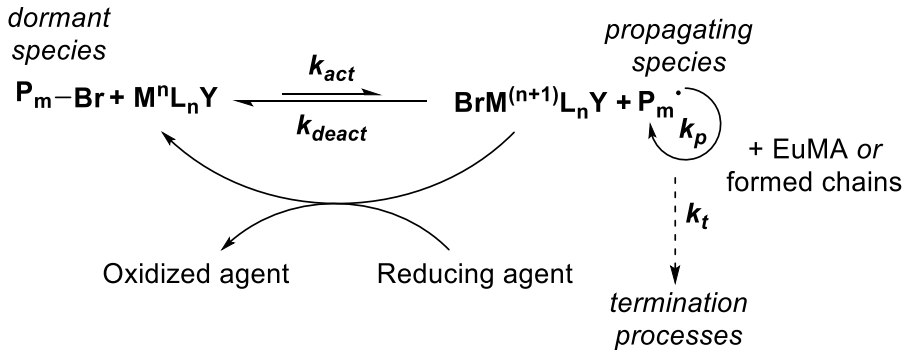

Scheme 3. Activation-deactivation mechanism of the catalyst complex in ARGET-ATRP. $K_{ATRP} = k_{act}/k_{deact}$. P_m═**P1**, **P2** or **P3**.

fact, the reaction

$$\mathbf{P1} - Br + \mathbf{P2} \rightarrow \mathbf{P1} + \mathbf{P2} - Br$$

presents a positive energy change (by 5.1 kcal/mol, estimated with DFT) due to a lower BDE for **P2**–Br. This result agrees with what indicated previously [19]. However, the addition of **P2** to **EuMA** requires surmounting higher barriers (9.9 and 13.9 kcal/mol, see Scheme 3) than the one predicted for the methacrylic radical (0.5 kcal/mol) or even **P1**, whose electronic structure is closely related to the one of the former. In terms of transition state theory, the relative importance of two reaction channels competing for the common reactant (i.e. methacrylic radical/**P1** or **P2** with **EuMA**) ought to be gauged by the total energy change from the dormant species to the TS's, the lowest of which being likely to dominate the overall reactivity. Thus, adding the BDE for the dormant species with the energy barriers, one notices that the reaction of the methacrylic radical **EuMA** is far more likely than the one involving **P2**.

In the end, ATRP-like processes may, indeed, reduce the formation of parasitic reactions responsible for the formation of branched or, even, crosslinked polymers, and it should do so especially when coupled with relatively low temperatures. In the latter cases, however, one may need to use ligands that increase the activator ability to generate radicals to maintain an acceptable polymerization kinetics.

It is worth recalling that the activity of the ATRP catalyst (and so the amount of radicals generated) is related to the redox behavior of the metal center (the lower the reducing potential the higher the activity, as it becomes more facile for Cu to be oxidized); the latter can be tuned by ligands, so that we deemed important investigating, in this work, the effect of a few of the latter with respect to the catalyst activity and to the side reactions that might involve the allyl group in the polymerization of **EuMA**. This task was only partially tackled in previous works involving monomers with cross-linkable groups, so that additional investigations appear worthy.

Unlike the classical ATRP, in the variant ARGET-ATRP the metal is added in its higher oxidation state, and it is continuously reduced by an exogenous reducing agent (i.e. $Sn(oct)_2$). This mechanism permits the introduction of the metal in its most stable oxidation state and, more importantly, the continuous regeneration of the catalytically active species ($\mathbf{M^n}XL_n$) allows for low catalyst loadings. Because of these characteristics, ARGET-ATRP is particularly tolerant towards oxygen and the products do not need purification from catalyst ashes, a very important aspect with respect to the environmental impact of the synthetic process. Besides, the low amount of catalyst limits the concentration of reactive radicals lowering the chance of side reactions involving halogenated species, that are more difficult to reactivate. Due to the latter aspect, we decided to apply ARGET rather than the classical ATRP for the **EuMA** radical polymerization.

Four commercially available amines, namely BiPy, PMDETA, HMTETA and Me_6TREN (Fig. 1), were chosen as bidentate, tridentate and tetradentate ligands for copper (II) bromide. As reported by Matyjaszewski and co-workers, the Cu(II)-based complexes formed by those ligands exhibit the following activity in classical ATRP: Me_6TREN ≫> PMDETA > HMTETA > Bipy. However, this trend can significantly be influenced by the nature of the solvent, initiator and monomer [20–33].

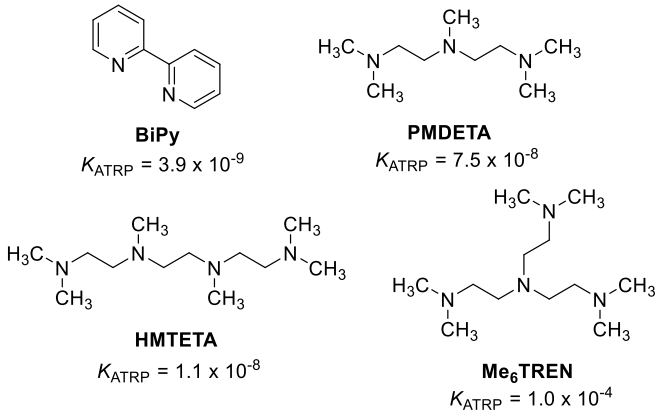

Fig. 1. Ligands employed in this investigation [17].

EuMA was synthesized by esterification of eugenol with methacrylic anhydride and DMAP at a relatively low temperature (45 °C) [15], and isolated in good yields (>80 %). This synthetic approach employing a safe anhydride proved more sustainable than previously reported methodologies requiring highly toxic chemicals such as methacroyl chloride [34].

EuMA polymerization was next investigated in the presence of EBIB as radical initiator. To reduce the extent of secondary reactions, all tests were carried out in solvent (anisole) rather than in bulk and at rather low temperature (60 °C), in the presence of the FDA approved tin (II) 2-ethylhexanoate ($Sn(oct)_2$) as the reducing agent. The monomer conversion, the molecular mass and polydispersity of polymers obtained at different polymerization times for each catalyst system are reported in Table 1 [35].

For reaction times up to 30 min, soluble polymers were attained with all catalytic systems; at this time, the highest monomer conversion (ca 50 %) was achieved in the presence of HMTETA (entry 4). The polymer proved completely soluble in organic solvents (anisole, dichloromethane, chloroform) and a preservation of the allyl moiety of 95 ± 3 % was confirmed by ^{1}H NMR spectroscopy. More in general, after 30 min of polymerization, the methacrylic-methacrylic propagation is still prevailing with respect to the formation of **P2** and **P3** for all the systems considered. However, the slight increase of polydispersity over the time, particularly evident for catalytic systems with Me_6TREN, HMTETA and BiPy, suggested that side reactions start becoming competitive upon consuming methacrylic functions.

Indeed, for polymerization times longer than 30 min, the $CuBr_2$/HMTETA and $CuBr_2$/BiPy systems generated partially insoluble, gel-like, products [37]. The formation of gel, indicative of the occurrence of crosslinking, was observed concurrently with an increase of viscosity of the reaction medium that probably reduced the diffusion of the monomer. Such factor, along with the lower concentration of unreacted methacrylic moiety, would favor the addition of the propagating radical species to inter and/or intra-chain allyl pedant groups (see mechanism of formation of **P3** in Scheme 2), or the transfer of the radical center from the methacrylic species to the allyl group (see mechanism of formation of **P2** in Scheme 2). After 360 min the polymer obtained in presence of HMTETA proved completely insoluble in organic solvents, indicating a higher degree of crosslinking.

Upon employing Me_6TREN and PMDETA as the ligands, no gelation/crosslinking was observed regardless of the reaction time, and soluble materials were obtained in all cases. Although the polymers isolated in the presence of Me_6TREN exhibited M_n somewhat higher than those obtained in the case of PMDETA, the latter allowed for narrower $Đ$ values (1.1–1.5 vs 1.2–1.8 for PMDETA and Me_6TREN, respectively), indicating a higher degree of control over the polymerization despite the lower activity of the catalyst system. Albeit the comparison between the K_{ATRP} of such two ligands would suggest a reverse trend of polymerization kinetics, the higher stabilization of Cu(II) species in the presence of Me_6TREN in allegedly leading to slower activation rate due to the inefficient initial reduction of Cu(II) to Cu(I) by the reducing agent. Finally, the comparison between theoretical- and calculated M_n indicated incomplete EBIB activation at all reaction times ($M_n > M_{n(theo)}$) upon using BiPy and Me_6TREN as the ligands, while this was observed only during the early stages of the polymerization (5 and 10 min) in the presence of PMDETA and HMTETA. Nevertheless, it has to be noted that experimental values have been determined against polystyrene standards and could not be corrected with an appropriate Mark-Houwink coefficient, hence the comparison should be intended only as trend-wise.

The kinetic graph relative to the polymerization of **EuMA** with

Table 1
ARGET-ATRP of **EuMA** catalyzed by $CuBr_2$/L (L = Me_6TREN, BiPy, HMTETA, PMDETA) systems.

Entry	Time (min)	Me_6TREN				PMDETA				HMTETA				BiPy			
		Conv. (%)[a]	M_n (theo) (kDa)[b]	M_n (kDa)[c]	Đ[c]	Conv. (%)[a]	M_n (theo) (kDa)[b]	M_n (kDa)[c]	Đ[c]	Conv. (%)[a]	M_n (theo) (kDa)[b]	M_n (kDa)[c]	Đ[c]	Conv. (%)[a]	M_n (theo) (kDa)[b]	M_n (kDa)[c]	Đ[c]
1	5	5	0.85	5.1	1.22	10	1.8	4.8	1.17	16	2.9	5.0	1.23	8	1.5	4.9	1.25
2	10	14	2.3	6.5	1.26	23	3.9	5.9	1.17	24	4.1	6.5	1.29	15	2.6	7.6	1.29
3	15	20	3.4	7.8	1.32	26	4.4	6.3	1.19	31	5.2	7.5	1.40	24	4.1	8.8	1.39
4	30	30	5.1	9.7	1.4	39	6.5	7.5	1.24	49	8.2	10.2	1.55	40	6.7	11.5	1.56
5	60	37	6.3	10.9	1.47	50	8.3	8.9	1.32	63[d]	10.4	11.5	1.91	51[d]	8.5	13.9	1.95
6	12	46	7.8	13.2	1.64	58	9.6	9.1	1.47	73[d]	12.0	13.4	2.53	56[d]	9.3	14.8	2.17
7	240	47	8.0	12.8	1.65	58	9.6	9.1	1.47	68[d]	11.3	8.2	2.10	57[d]	9.5	15.4	2.23
8	360	54	9.2	14.1	1.85	57	9.5	9.1	1.47	n.d.[d]	n.d.	n.d.	n.d.	58[d]	9.6	16.1	2.13

Reaction conditions: **EuMA** (1.0 g, 4.3 mmol), anisole 1.0 mL (50/v/wt%); **EuMA**/EBIB/$CuBr_2$/Ligand/$Sn(oct)_2$: 400/10/1/2/2, T = 60 °C. n.d = not determined.
[a] Determined by ^{1}H NMR spectroscopy on the crude reaction mixture [36].
[b] Calculated from ($[\mathbf{EuMA}]_0$ /$[EBIB]_0$)x conv.x Mw(**EuMA**) + Mw(**EBIB**)
[c] Determined by GPC against PS standards.
[d] Formation of gels [37].

PMDETA-based catalyst showed that the monomer conversion reached a *plateau* at ca. 60 % (Fig. 2b). Such *plateau* could, tentatively, be ascribed to chain termination processes, a hypothesis reinforced by observing that neither the M_n nor the Đ of the P(**EuMA**)s significantly changed for reaction times longer than 120 min, that is after reaching the highest monomer conversion (Fig. 2a). On the other hand, a progressive increase of M_n as well as the broadening of the distribution was observed during the early stages of the polymerization (5–60 min). This evidence suggested the involvement of pendant allyl moieties in termination processes, or, at least, in the slowing down of the polymerization kinetics.

To experimentally confirm the involvement of the allyl group, the polymerization of the allyl-hydrogenated monomer, dihydrogen eugenyl methacrylate (**DEuMA**), was carried out under the same reaction conditions [38,39]. Interestingly, in this case no conversion *plateau* was observed, and more than 80 % conversion was attained within 6 h of polymerization (Fig. 2b).

Evidence of the participation of the allyl group to, possibly, termination and alternative processes with the PMDETA based system were obtained by analysis of the ^{13}C NMR spectrum of the P(**EuMA**) isolated after 360 min (Fig. 3a). The resonances at 38.8, 41.5 and 41.9 ppm indicated the addition of the methacrylic radical to an allyl group generating **P3** (Scheme 2), the structure of which being also indicated in the figure. The same signals were, instead, not observed in the spectrum of the polymer isolated after 30 min (Fig. 3b), suggesting the non-occurrence (or non-detectability, at least) of such process involving the allyl group during the early stages of polymerization. The absence of such signals for polymer obtained with catalyst based on HMTETA (Fig. 3c) is probably due to the fact that we analyzed only the organic soluble fraction of the product, since the gelation was already started (see entry 5 in Table 1). According to the discussion provided in the computational section, the attack of the methacrylic radical to the allyl double bond generating the brominated **P3**–Br produces a species less

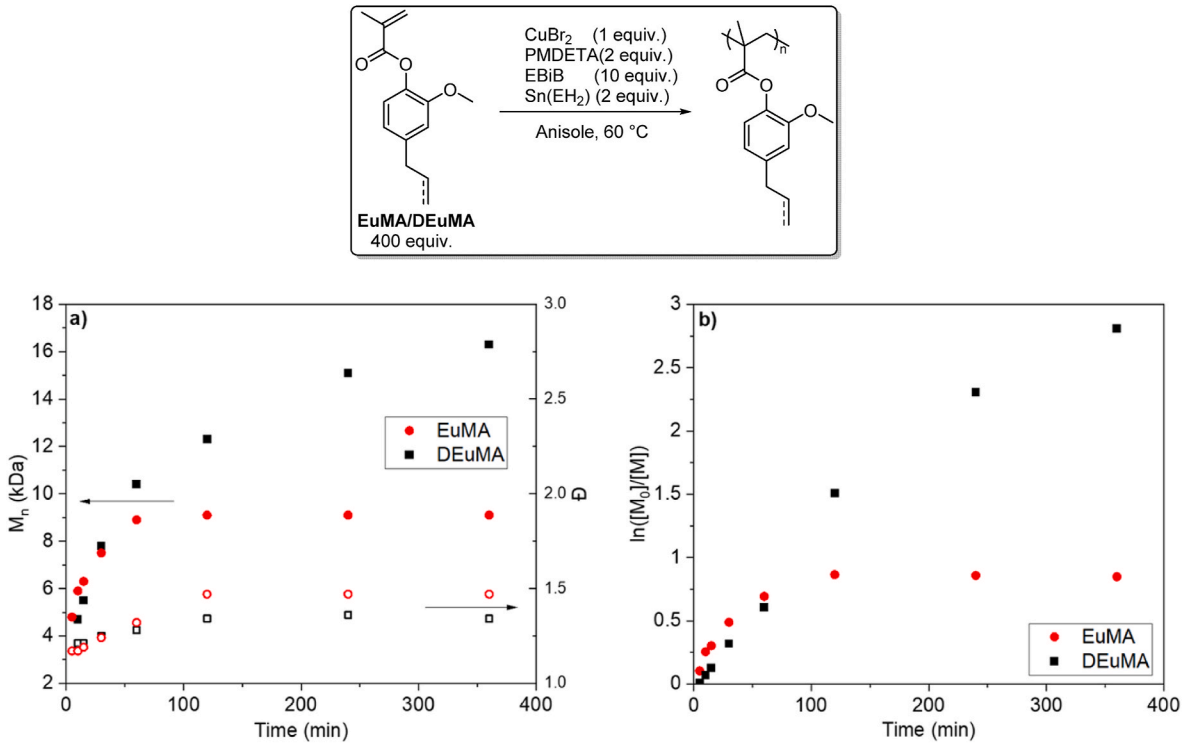

Fig. 2. ARGET-ATRP of **EuMA** and **DEuMA** in presence of $CuBr_2$/PMDETA at 60 °C in anisole (monomer/EBIB/$CuBr_2$/Ligand/$Sn(oct)_2$ **400/10/1/2/2**): dependency of M_n and Đ of P(**EuMA**) and P (**DEuMA**) on the reaction time (a); comparison between the conversion rates of **EuMA** and **DEuMA** (b).

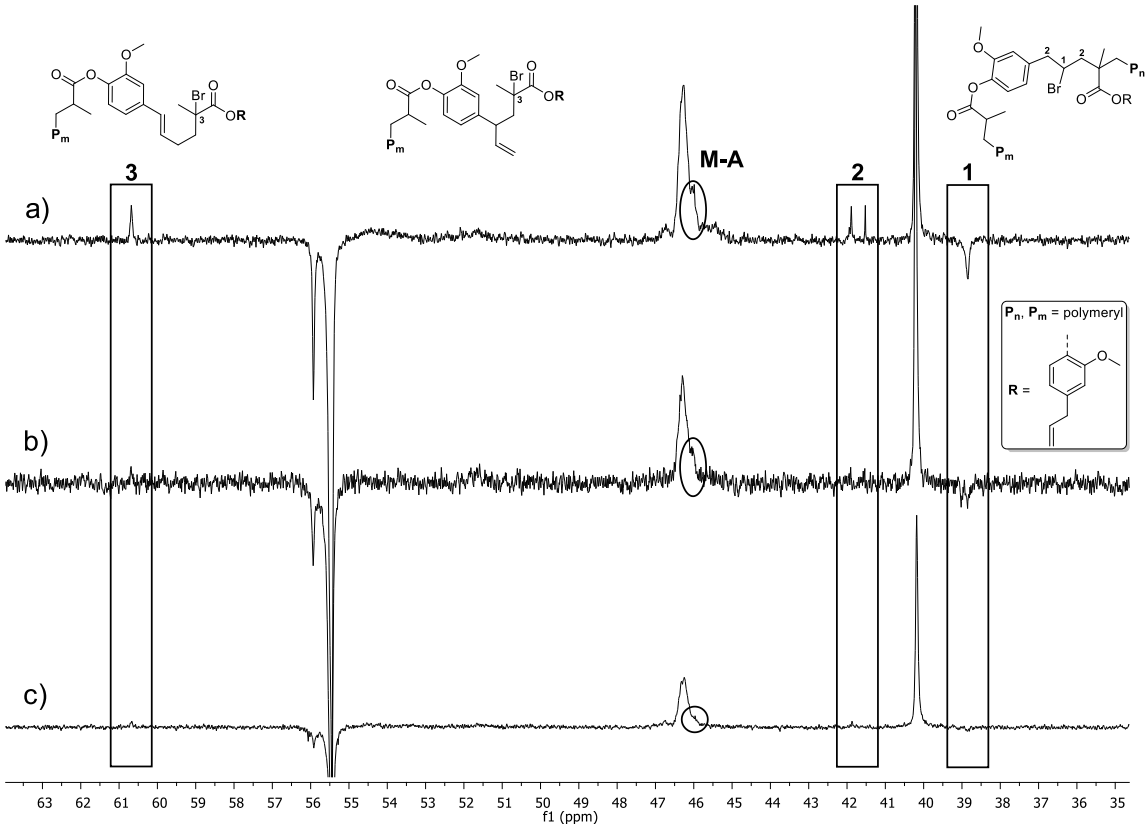

Fig. 3. Comparison between the ^{13}C-{^{1}H} NMR spectra (100 MHz, $CDCl_3$, 25 °C) of P(**EuMA**) samples obtained with: $CuBr_2$/PMDETA after 360 min (a, top) and 30 min (b, middle) and with $CuBr_2$/HMTETA after 60 min (c). The rectangles indicate signals relative to inactivated, brominated specie P3 and P2a P2b. Reaction conditions: anisole, 60 °C, **EuMA**/EBIB/$CuBr_2$/Ligand/Sn(oct)$_2$: **400/10/1/2/2**.

likely to be reactivated due to its secondary nature.

In addition to what discussed so far, the signal at ca 60 ppm in spectrum 3a was attributed to the quaternary carbon of **P2a** and/or **P2b** (See the Supporting Information) dormant specie (i.e. linked to a bromide atom), being the rest of the structure almost superimposable with that of the polymer. Indeed, the presence of a broad signal in the range 45.5–47 ppm, assigned to the Methacryl-Allyl (M-A) sequences and indicative of a possible irregular chain-propagation deriving from the addition of the allyl radical to a methacrylic group generating propagating species, was also observed, while signals relative to the Allyl-Allyl (A-A) sequences at 35–39 ppm were absent (see the Supporting Information, Fig. S11) [40]. We could thus infer that, overall, the NMR results shown in Fig. 3a and b support the conclusion drawn from electronic structure results, and, hence, suggest that the motivation behind our attempt were indeed robust.

All the reported observations, the absence of gelation and the solubility of the isolated polymers in the Cu(II)/PMDETA case being key, suggested that a rationalization for the different behaviors could be found in the possibility that $CuBr_2$/PMDETA gave a lower concentration of reacting radicals (and thus of the likelihood of side reactions) than BiPy- and HMTETA-based catalysts, the latter difference being related to a lower Cu(I)/Cu(II) ratio present with PMDETA. This idea would be in accord with previous observations such as the fact that.

1. according to Matyjaszewski [21], PMDETA is more active in ATRP than the other two ligands, as it better stabilizes the higher oxidation state of copper. Conversely, the presence of the active species Cu(I) should be lower when the same ligand is employed during ARGET-ATRP compared to BiPy and HMTETA cases with all remaining conditions left unchanged, as it produced from Cu(II) by an equilibrated redox with the Sn(II)/Sn(IV) pair.
2. The values of K_{ATRP} provided in Ref. [17] allow one to estimate that the equilibrium constant for the reaction (L_1 = PMDETA) $Cu(I)BrL_1 + Cu(II)Br_2L_2 \leftrightarrows Cu(II)Br_2L_1 + Cu(I)BrL_2$ is, roughly, 10 and 40 when L_2 is, respectively, HMTETA and BiPy. Such results indicate a 4 and 7-fold higher concentration of Cu(I) species in the latter cases, which clearly support the idea of more active, hence less selective, catalytic systems.

In the end, according to Equation (1) [41]

$$R_p = k_p\, K_{ATRP}\, \frac{[RX][Cu(I)]}{[Cu(II)]}\, [M] \qquad (1)$$

the rate of all radical reactions involved in the polymerization ought to be increased upon increasing the [Cu(I)]/[Cu(II)] ratio, so that the faster increase of molecular masses and dispersity observed in the presence of HMTETA and BiPy-based species compared to the PMDETA case may be explained by this single effect. This notwithstanding, we consider also worth mentioning that one could conceive the mentioned differences in behavior as related to the fact that, all other conditions remaining the same, the higher Cu(II) concentration present when more stabilizing ligands (i.e. PMDETA and Me_6TREN) are used would make the deactivation reaction faster, thus reducing the active radical concentration. This kinetic argument is, however, already encompassed in the thermodynamics-based analysis presented above, as both activation and deactivation are elementary processes playing a role in defining K_{ATRP} or derived equilibrium constants.

Apparently, neither 3a nor 3c spectra displayed indications for the presence of A-A sequences. This notwithstanding, the presence in the

chains of M-A sequences suggested that the radical generated via addition onto the double bond of the allyl group could undergo chain propagation reactions, but only if in presence of more reactive double bonds than its own. To verify this idea, polymerization tests of eugenol acetate (**EuAc**) [42] with the $CuBr_2$/PMDETA system under the reaction conditions employed for **EuMA** were carried out. No polymer formation was attained even after prolonged reaction times (24 h). The experimental observation did not exclude the formation of very short A-A sequences; however, it represents a proof that extended A-A propagation is generally hampered. In spite of this, the reaction of equimolar amounts of **EuAc** and EBIB in the presence of the $CuBr_2$/BiPy catalyst (which appeared active in inducing undesired side-reactions) afforded the adduct arising from the addition of the ethyl isobutyrate radical to the allyl group of the monomer [43], demonstrating some activity for the reactive channel leading to **P3**. Based on these results, it was tentatively proposed that, albeit possible, chain propagation through the allyl-derived radical occurs to a much lower extent than the elongation involving methacrylic radicals.

As discussed earlier, the conversion of **EuMA** in the presence of $CuBr_2$/PMDETA proved linear for short reaction times (<60 min) before reaching a plateau despite the secondary reactions. As highlighted by both experiments and our computational studies, this trend could be ascribed to the involvement of the allyl group in the chain propagation and/or termination processes eventually deactivating the catalyst system. Such deactivation could either be caused by accumulation of Cu(II)-based species or by the complete depletion of the catalyst-regenerating reducing agent. In order to assess which of these factors limited the **EuMA** conversion, experiments involving the introduction of either freshly prepared Cu(II)/PMDETA system or additional $Sn(oct)_2$ to a polymerization process still exhibiting linear conversion behavior, were carried out. The amount of catalyst and reducing agent employed in these tests corresponded to those used at the beginning of the polymerization process (1 equiv. and 2 equiv., respectively). Data reported in Fig. 4 indicated that in both cases the introduction of exogenous reactants after 60 min of reaction (see vertical marker) improved the monomer conversion. However, the reducing agent strongly enhanced the reaction kinetics leading to the formation of gels within 2 h; no insoluble products were attained, instead, after the addition of freshly prepared Cu(II)-based system despite the observed boost of the reaction kinetics. These results suggested that the conversion plateau was

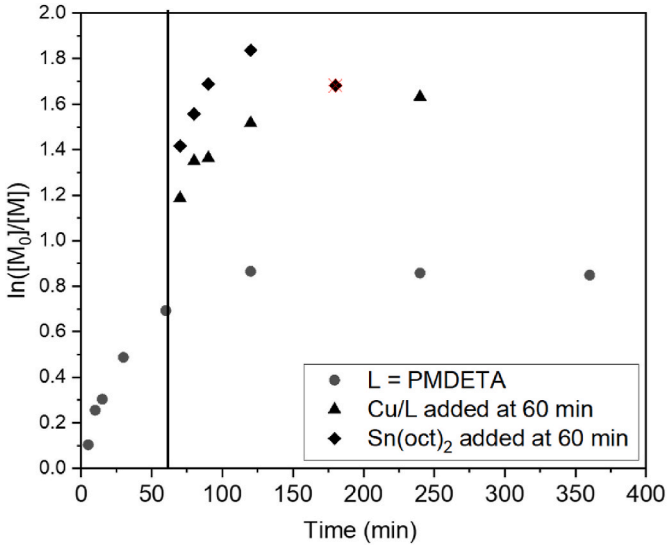

Fig. 4. Kinetic plot of **EuMA** polymerization in the presence of PMDETA (filled circles) and its variation upon addition of 1eq of $CuBr_2$/PMDETA (filled triangles) or $Sn(oct)_2$ (filled diamonds) after reaching the conversion plateau at 60 min. The marked (x) point indicates the formation of gels.

primarily caused by accumulation of Cu(II) that could no longer be reduced due to the progressive consumption of $Sn(oct)_2$, a process leading to the decrease of the concentration of redox products. The test involving the fleshly added Cu(II)-base species, in fact, indicated the presence of residual $Sn(oct)_2$ still able to regenerate, although rather ineffectively, the catalyst system due to the consequence of Le Chatelier-Braun principle following the addition of Cu(II). The quantitative difference between the two tests may easily be ascribed to the stoichiometry of the redox reaction, which generates two Cu(I) ions for every Sn(II) reacted. In the end, the involvement of the Cu(I)/Cu(II) ratio in defining the fate of the reacting system appears clearly.

The higher stability of Cu(II) and its accumulation, when coordinated with PMDETA rather than to HMTETA or BiPy, is however just one facet of a complicate reaction system. In fact, the catalyst deactivation may tentatively be attributed, at least in part, to termination reactions via either coupling of two active radical chains or their disproportionation, as also evidenced by the NMR spectroscopy analysis discussed above. The termination processes would leave the catalytic Cu in the oxidized state bearing two bromine atoms. Obviously, this result leads to the usage of more $Sn(oct)_2$ and, consequently to a decrease of its concentration. The presence of the allyl group, and the increasing chance for the reaction leading to **P2** to take place following **EuMA** consumption, should facilitate radical coupling. In fact, a **P2**-like species may be more easily regenerated from its brominated counterparts than from **P1**–Br or **P3**–Br (*vide supra* for an energetic comparison), with the net effect of generating a higher concentration of non-propagating radicals (see Scheme 3 for TS barriers), which are however capable of coupling and, perhaps, disproportionation. The latter observation appears to rationalize the different behavior of conversion of **DEuMA** compared with **EuMA**, the former being less prone to generate easily reactivated but non-reactive species with bromine atoms in position 1 on the pendant due to the missing double bond and, consequently, stabilization via resonance, as can be seen from the energy change for the reaction (**P2_idrog** being the allyl hydrogenated counterpart of **P2**):

$$\mathbf{P2} - Br + \mathbf{P2\_}\boldsymbol{idrog} \rightarrow \mathbf{P2} + \mathbf{P2\_}\boldsymbol{idrog} - Br$$

that is predicted to be −7.4 kcal/mol. Interestingly, the much higher polydispersity seen when using the HMTETA and BiPy ligands may also been favored by a higher concentration of **P2**-like radicals relative to **P1**-like ones compared to the PMDETA case, the former being substantially only prone to termination reactions as discussed above.

To further reduce the secondary radical reactions, polymerization tests at lower copper catalyst loading (500 vs the original 2500 ppm) were carried out. A drastic decrease of the reaction rate was observed regardless of the ligand employed (Table 2, entries 1 and 2). Nevertheless, upon increasing the amount of reducing agent (10 vs the original 2 equiv.), improvement of the monomer conversion was attained (Table 2, entries 3–5), albeit gel formation was obtained at *circa* 50 % conversion; this suggests loss of control over the radical generation, in accordance with the previous observations (*vide supra*). In particular, data relative to the $CuBr_2$/PMDETA catalyst suggested a delicate

Table 2
ARGET-ATRP of **EuMA** catalyzed by 500 ppm of $CuBr_2$/L (L = BiPy, PMDETA) systems.

Entry	Time (h)	$CuBr_2$/PMDETA	$CuBr_2$/BiPy	EuMA/EBIB/$CuBr_2$/Ligand/$Sn(oct)_2$
		Conversion (%)	Conversion (%)	Molar ratios
1	4	9	3	**2000**/10/1/2/**2**
2	8	11	4	
3	0.5	25	9	**2000**/10/1/2/**10**
4	1	30	11	
5	2	51[a]	55[a]	

[a] Formation of gel.

balance between Cu(I)/Cu(II) ratio and the monomer concentration for the massive involvement of the allyl group in the propagation process.

In principle, the linearity of ln ([M_0]/[M]) vs time should indicate that the system $CuBr_2$/PMDETA promoted the living polymerization of **EuMA** at least up to 50 % of conversion. To prove this assumption, a P **(EuMA)** sample obtained after 30 min of polymerization (Table 1, entry 3), when the inactive species generated by secondary reactions are negligible, was used as the macroinitiator in the ARGET ATRP of methyl methacrylate (**MMA**). The formation of a block copolymer was confirmed by both GPC, that showed a shift of the macroinitiator to higher molecular masses (see the Supporting Information, Fig. S16), and by the DOSY-NMR spectroscopy (see the Supporting Information, Fig. S17) where the alignment of signals of macroinitiator and the P (**MMA**) block indicated they are part of the same polymer chain.

4. Conclusions

Over the last decade, increasing attention has been devoted to the development of sustainable polymers that, while exhibiting properties similar to that of common commodity plastics, satisfy the need for reducing our dependency on fossil-based raw materials. Natural phenolic molecules have emerged as promising building blocks for renewable monomers. In this scenario, eugenol (**Eu**) proved an excellent candidate for the development of novel sustainable materials. Indeed, aside from being ubiquitous in nature, **Eu** can be obtained from biomass valorization such as lignin depolymerization and exhibits additional properties such as antioxidant, antiseptic and antimicrobial activity. Moreover, its allyl group, if preserved during the polymerization process, would serve as post-functionalization site to produce more advanced materials for tailored applications, especially when being part of block co-polymeric species. Despite its poor reactivity towards radical polymerization, the said allyl function still proved to be involved in secondary reactions leading to insoluble/crosslinked materials or polymers with high broad molecular masses distribution. In this work, we used the controlled radical polymerization ARGET-ATRP catalyzed by $CuBr_2$/BiPy, $CuBr_2$/HMTETA and $CuBr_2$/PMDETA systems to study theoretically and experimentally the polymerization of the methacrylic derivative of eugenol, namely eugenyl methacrylate (**EuMA**), focusing the attention on the side reactions occurring in presence of the adopted catalyst system. Starting from the theoretical approach, our calculations provided a complete and an in-depth overview of the energetic of species deriving from the radical chain transfer to the allyl group through hydrogen abstraction (**P2**), as well as from the attack of the propagating methacrylic radical to the allyl group (**P3**). **P2**, **P3**, and their derivatives, can be easily formed during the radical polymerization, since their energetic barriers are, indeed, higher, but still comparable to that of methacrylic-methacrylic propagation. The experimental behavior of the three different Cu(II)-based catalysts in the ARGET-ATRP indicated that the Cu(I)/Cu(II) ratio was the key to control the formation of **P2**, **P3** and their derivatives, and that the catalyst system based on PMDETA as ligand was able to form soluble polymers at higher conversion by inactivating the catalyst system via the reducing agent consumption rather than by the formation of insoluble/crosslinked polymers. This was due to the inactivity of P2 and P3 brominated species and the rationalization of such a behavior was attributed to the lower amount of the starting inactive Cu(II) complex reduced to the Cu(I) active catalyst promoted by the PMDETA. In fact, when increasing the reducing agent, and consequently the Cu(I)/Cu(II) ratio, even in presence of larger amount of monomer, cross-linked occurred for the increasing concentration of radical species.

The living character of polymerization was confirmed using P (**EuMA**), obtained in the range of linearity of the monomer conversion, as macroinitiator in the **MMA** polymerization. This experiment represents a proof of concept that would pave the way to the synthesis of novel, block-type, multifunctional as well as post-functionalized materials. Indeed, the latter goal is not easily reached when employing free radical polymerization, as chemical nature does not allow to conserve chain end activity. In conclusion, although the right modulation of all the experimental conditions is not trivial, the ARGET-ATRP allows the synthesis of polymers based on eugenol with monomodal distribution of molecular weight, with active terminal chain and preserving the allyl groups.

More in general, our study demonstrated that a fine modulation of the kinetic of polymerization by ligands, and hence Cu(I)/Cu(II) ratio, together with low temperatures of polymerization, can be used to reduce secondary reactions of molecules with sensitive functional groups such as those deriving from renewable sources.

CRediT authorship contribution statement

Aniello Vittore: Validation, Investigation. **Orlando Santoro:** Visualization, Project administration, Methodology. **Mirko Candida:** Validation, Investigation. **Stefano Vaghi:** Investigation. **Stefania Pragliola:** Visualization. **Massimo Mella:** Writing – review & editing, Writing – original draft, Visualization, Resources, Project administration, Methodology, Funding acquisition, Formal analysis, Conceptualization. **Lorella Izzo:** Writing – review & editing, Writing – original draft, Visualization, Supervision, Resources, Project administration, Methodology, Funding acquisition, Conceptualization.

Declaration of competing interest

The authors declare that they have no known competing financial interests or personal relationships that could have appeared to influence the work reported in this paper.

Acknowledgments

AV and SV thank Ministero dell'Università e della Ricerca (MUR) (DM 1061/2021) and Università degli Studi dell'Insubria, respectively, for a postgraduated studentship. OS thanks the support by MUR (DM 1062/2021). LI and MM thank Università degli Studi dell'Insubria for funding under the scheme Fondo d'Ateneo per la Ricerca (FAR 2023). SP thanks MUR for funding under the scheme Progetti di Rilevante Interesse Nazionale PRIN2020 (2020EZ8EPB).

Appendix A. Supplementary data

Supplementary data to this article can be found online at https://doi.org/10.1016/j.polymer.2025.128228.

Data availability

Data will be made available on request.

References

[1] A.A. Khalil, U.U.R. Rahman, M.R. Khan, A. Sahar, T. Mehmood, M. Khan, Essential oil eugenol: sources, extraction techniques and nutraceutical perspectives, RSC Adv. 7 (2017) 32669, https://doi.org/10.1039/C7RA04803C.
[2] L. Wang, R. Zhang, J. Li, L. Guo, H. Yang, F. Ma, H. Yu, Comparative study of the fast pyrolysis behavior of ginkgo, poplar, and wheat straw lignin at different temperatures, Ind. Crops Prod. 122 (2018) 465, https://doi.org/10.1016/j.indcrop.2018.06.038.
[3] R. Morales-Cerrada, S. Molina-Gutierrez, P. Lacroix-Desmazes, S. Eugenol Caillol, A promising building block for biobased polymers with cutting-edge properties, Biomacromolecules 22 (2021) 3625, https://doi.org/10.1021/acs.biomac.1c00837.
[4] S. Caillol, B. Boutevin, R. Auvergne, Eugenol, a developing asset in biobased epoxy resins, Polymer 223 (2021) 123663, https://doi.org/10.1016/j.polymer.2021.123663.
[5] L. Rojo, B. Vazquez, J. Parra, A. Lopez Bravo, S. Deb, J. San Roman, From natural products to polymeric derivatives of "eugenol": a new approach for preparation of dental composites and orthopedic bone cements, Biomacromolecules 7 (2006) 2751, https://doi.org/10.1021/bm0603241.

[6] J. Deng, B. Yang, C. Chen, J. Liang, Renewable eugenol-based polymeric oil-absorbent microspheres: preparation and oil absorption ability, ACS Sustainable Chem. Eng. 3 (2015) 599, https://doi.org/10.1021/sc500724e.

[7] S. Molina-Gutierrez, V. Ladmiral, R. Bongiovanni, S. Caillol, P. Lacroix-Desmazes, Emulsion polymerization of Dihydroeugenol-, eugenol-, and isoeugenol-derived methacrylates, Ind. Eng. Chem. Res. 58 (2019) 21155, https://doi.org/10.1021/acs.iecr.9b02338.

[8] S. Molina-Gutierrez, S. Dalle Vacche, A. Vitale, V. Ladmiral, S. Caillol, R. Bongiovanni, P. Lacroix-Desmazes, Photoinduced polymerization of eugenol-derived methacrylates, Molecules 25 (2020) 3444, https://doi.org/10.3390/molecules25153444.

[9] R. Ding, Y.Y. Du, R.B. Goncalves, L.F. Francis, T.M. Reineke, Sustainable near UV-curable acrylates based on natural phenolics for stereolithography 3D printing, Polym. Chem. 10 (2019) 1067, https://doi.org/10.1039/C8PY01652F.

[10] S. Molina-Gutierrez, A. Manseri, V. Ladmiral, R. Bongiovanni, S. Caillol, P. Eugenol Lacroix-Desmazes, A promising building block for synthesis of radically polymerizable monomers, Macromol. Chem. Phys. 220 (2019) 1900179, https://doi.org/10.1002/macp.201900179.

[11] N.G.J. Gaylord, Allyl polymerization. IV. Effective chain transfer in polymerization of allyl monomers, Polym. Sci. 22 (1956) 71, https://doi.org/10.1002/pol.1956.1202210010.

[12] Y. Zhang, M.A. Dubè, E. Vivaldo-Lima, Modeling degradative chain transfer in d-Limonene/n-Butyl methacrylate free-radical copolymerization, J. Renew. Mat. 3 (2015) 318, https://doi.org/10.7569/JRM.2015.634115.

[13] C.A. Barson, J.C. Bevingtont, B.J. Bunt, The effects of some phenyl derivatives of propene upon radical polymerizations, Polymer 39 (1998) 1345, https://doi.org/10.1016/S0032-3861(97)00463-1.

[14] X. Pan, M. Fantin, F. Yuan, K. Matyjaszewski, Externally controlled atom transfer radical polymerization, Chem. Soc. Rev. 47 (2018) 5457, https://doi.org/10.1039/C8CS00259B.

[15] J.F. Stanzione, J.M. Sadler, J.J. La Scala, R.P. Wool, Lignin model compounds as bio-based reactive diluents for liquid molding resins, ChemSusChem 5 (2012) 1291, https://doi.org/10.1002/cssc.201100687.

[16] Gaussian 09, Revision B.01, Frisch, M. J.; Trucks, G. W.; Schlegel, H. B.; Scuseria, G. E.; Robb, M. A.; Cheeseman, J. R.; Scalmani, G.; Barone, V.; Mennucci, B.; Petersson, G. A.; Nakatsuji, H.; Caricato, M.; Li, X.; Hratchian, H.P.; Izmaylov, A. F.; Bloino, J.; Zheng, G.; Sonnenberg, J. L.; Hada, M.; Ehara, M.; Toyota, K.; Fukuda, R.; Hasegawa, J.; Ishida, M.; Nakajima, T.; Honda, Y.; Kitao, O.; Nakai, H.; Vreven, T.; Montgomery Jr., J. A.; Peralta, J. E.; Ogliaro, F.; Bearpark, M.; Heyd, J. J.; Brothers, E.; Kudin, K. N.; Staroverov, V. N.; Kobayashi, R.; Normand, J.; Raghavachari, K.; Rendell, A.; Burant, J. C.; Iyengar, S. S.; Tomasi, J.; Cossi, M.; Rega, N.; Millam, J. M.; Klene, M.; Knox, J. E.; Cross, J. B.; Bakken, V.; Adamo, C.; Jaramillo, J.; Gomperts, R.; Stratmann, R. E.; Yazyev, O.; Austin, A. J.; Cammi, R.; Pomelli, C.; Ochterski, J. W.; Martin, R. L.; Morokuma, K.; Zakrzewski, V. G.; Voth, G. A.; Salvador, P.; Dannenberg, J. J.; Dapprich, S.; Daniels, A. D.;Farkas, O.; Foresman, J. B.; Ortiz, J. V.; Cioslowski, J.; Fox, D. J. Gaussian, Inc., Wallingford CT, 2009.

[17] W. Tang, Y. Kwak, W. Braunecker, N.V. Tsarevsky, M.L. Coote, K. Matyjaszewski, Understanding atom transfer radical polymerization: effect of ligand and initiator structures on the equilibrium constants, J. Am. Chem. Soc. 130 (2008) 10702, https://doi.org/10.1021/ja802290a.

[18] A.K.K. Fung, M.L. Coote, A mechanistic perspective on atom transfer radical polymerization, Polym. Int. 70 (2021) 918, https://doi.org/10.1002/pi.6130.

[19] C.Y. Lin, M.L. Coote, A. Gennaro, K. Matyjaszewski, Ab initio evaluation of the thermodynamic and electrochemical properties of alkyl halides and radicals and their mechanistic implications for atom transfer radical polymerization, J. Am. Chem. Soc. 130 (2008) 12762, https://doi.org/10.1021/ja8038823.

[20] A. Kaur, T.G. Ribelli, K. Schröder, K. Matyjaszewski, T. Pintauer, Properties and ATRP activity of copper complexes with substituted tris(2-pyridylmethyl)amine-based ligands, Inorg. Chem. 54 (2015) 1474, https://doi.org/10.1021/ic502484s.

[21] O. Santoro, M.C. Malacarne, F. Sarcone, L. Scapinello, S. Pragliola, E. Caruso, V. T. Orlandi, L. Izzo, Inherently antimicrobial P(MMA-ran-DMAEMA) copolymers sensitive to photodynamic therapy: a double bactericidal effect active wound dressing, Int. J. Mol. Sci. 24 (2023) 4330, https://doi.org/10.3390/ijms24054340.

[22] M. Mella, A. Tagliabue, G. Viscusi, G. Gorrasi, L. Izzo, How chemical structure and composition impact on the release of salt-like drugs from hydrophobic matrices: variation of mechanism upon adding hydrophilic features to PMMA, Colloids Surf. A Physicochem. Eng. Asp. 646 (2022) 128878, https://doi.org/10.1016/j.colsurfa.2022.128878.

[23] M. Mella, A. Tagliabue, S. Vaghi, L. Izzo, Evidences for charged hydrogen bonds on surfaces bearing weakly basic pendants: the case of PMMA–ran–PDMAEMA polymeric films, Colloids Surf. A Physicochem. Eng. Asp. 620 (2021) 126525, https://doi.org/10.1016/j.colsurfa.2021.126525.

[24] Y. Miele, M. Mella, L. Izzo, F. Rossi, Composition and microstructure of biocompatible and pH-sensitive copolymers prepared by a free solvent ARGET ATRP, Advances in Bionanomaterials II (2020) 3–15, https://doi.org/10.1007/978-3-030-47705-9_1.

[25] L. Izzo, G. Gorrasi, A. Sorrentino, A. Tagliabue, M. Mella, Controlling drug release of anti-inflammatory molecules through a pH-sensitive, bactericidal polymer matrix: towards a synergic and combined therapy, Adv. Biomater. II (2020) 167, https://doi.org/10.1007/978-3-030-47705-9_14.

[26] L. Izzo, S. Matrella, M. Mella, G. Benvenuto, G. Vigliotta, Escherichia coli as a model for the description of the antimicrobial mechanism of a cationic polymer surface: cellular target and bacterial contrast response, ACS Appl. Mater. Interfaces 11 (2019) 15332, https://doi.org/10.1021/acsami.9b02903.

[27] M. Mella, M.V. La Rocca, Y. Miele, L. Izzo, On the origin and consequences of high DMAEMA reactivity ratio in ATRP copolymerization with MMA: an experimental and theoretical study, J. Polym. Sci., Part A: Polym. Chem. 56 (2018) 1366, https://doi.org/10.1002/pola.29017.

[28] S. Villani, R. Adami, E. Reverchon, A.M. Ferretti, A. Ponti, M. Lepretti, I. Caputo, L. Izzo, pH-sensitive polymersomes: controlling swelling via copolymer structure and chemical composition, J. Drug Target. 5 (2017) 899, https://doi.org/10.1080/1061186X.2017.1363216.

[29] M.C. Barrella, A. Di Capua, R. Adami, E. Reverchon, M. Mella, L. Izzo, Impact of intermolecular drug-copolymer interactions on size and drug release kinetics from pH-responsive polymersomes, Supramol. Chem. 29 (2017) 796, https://doi.org/10.1080/10610278.2017.1377836.

[30] M. De Rosa, G. Vigliotta, A. Soriente, V. Capaccio, G. Gorrasi, R. Adami, E. Reverchon, M. Mella, L. Izzo, "Leaching or not leaching": an alternative approach to antimicrobial materials: via copolymers containing crown ethers as active groups, Biomater. Sci. 5 (2017) 741, https://doi.org/10.1039/C6BM00950F.

[31] S. Matrella, C. Vitiello, M. Mella, G. Vigliotta, L. Izzo, The role of charge density and hydrophobicity on the biocidal properties of self-protonable polymeric materials, Macromol. Biosci. 15 (2015) 927, https://doi.org/10.1002/mabi.201400503.

[32] G. Vigliotta, M. Mella, D. Rega, L. Izzo, Modulating antimicrobial activity by synthesis: dendritic copolymers based on non-quaternized 2-(dimethylamino)ethyl methacrylate by Cu-mediated ATRP, Biomacromolecules 13 (2012) 833, https://doi.org/10.1021/bm2017349.

[33] J. Lad, S. Harrisson, G. Mantovani, D.M. Haddleton, Copper mediated living radical polymerisation: interactions between monomer and catalyst, Dalton Trans. 4175 (2003).

[34] E. Boess, S. Karanestora, A.-E. Bosnidou, B. Schweitzer-Chaput, M. Hasenbeck, M. Klussmann, Synthesis of oxindoles by brønsted acid catalyzed radical cascade addition of ketones, Synlett 26 (2015) 1973, https://doi.org/10.1055/s-0034-1381052.

[35] Spectroscopic- and Thermal Analyses of Relevant Polymer Samples of P(**EuMA**) Are Reported in Figures S1-S3 of the Supporting Information.

[36] The Method Employed to Determine the Conversion of **EuMA** during the Polymerization Process by NMR Spectroscopy Is Shown in Figure S4 of the Supporting Information.

[37] Due to the partial insolubility of the products, monomer conversions as detected by ^{1}H-NMR spectroscopy could be underestimated. GPC Data Refer to the Soluble Fraction of the Sample.

[38] The Method Employed to Determine the Conversion of **DEuMA** during the Polymerization Process by NMR Spectroscopy Is Shown in Figure S5 of the Supporting Information.

[39] Spectroscopic- and Thermal Analyses of Relevant Polymer Samples of P(**DEuMA**) Are Reported in Figures S6-S9 of the Supporting Information.

[40] F. Heatley, P.A. Lovell, J. McDonald, NMR studies of free-radical polymerization and copolymerization of monomers and polymers containing allyl groups, Eur. Polym. J. 29 (1993) 255, https://doi.org/10.1016/0014-3057(93)90092-T.

[41] W. Tang, K. Matyjaszewski, Effect of ligand structure on activation rate constants in ATRP, Macromolecules 39 (2006) 4953, https://doi.org/10.1021/ma0609634.

[42] J.M. Álvarez-Calero, Z.D. Jorge, Massanet, $TiCl_4$/et_3N-mediated condensation of acetate and formate esters: direct access to β-alkoxy- and β-aryloxyacrylates, G. M. Org. Lett. 18 (2016) 6344, https://doi.org/10.1021/acs.orglett.6b03233.

[43] Albeit the $[M]^+$ could not be observed by EI-MS analysis, The Fragmentation Patter and the Molecular Masses of the Fragments Were in Agreement with Proposed Molecule (See the Supporting Information, Figures S12-S15).